Study on Evaluation and Prediction Model of Long-term Mechanical Properties of Fine-grained Saline Soil Subgrade

Ruheiyan Muhemaier[1,2] Mao Wei[2,*], Liu Xuejun[3], Xie Liangfu[1] and Ren Zulin[1]

[1]*Architectural Engineering Institute, Xinjiang University, Urumqi Xinjiang 830046, China*
[2]*School of Road and Bridge Engineering, Xinjiang Vocational and Technical College of Communications, Urumqi Xinjiang 831401, China*
[3]*Surveying and Geotechnical Division, Xinjiang Building Science Research Institute Co., LTD, Urumqi Xinjiang 830002, China*
E-mail: mw7397@126.com
[*]*Corresponding Author*

Received 17 July 2024; Accepted 01 September 2024

Abstract

In this thorough examination, we dive deep into the long-lasting mechanical characteristics of fine-grained saline soil subgrades, aspiring to establish a precise and reliable collection of predictive models. Our objective is to provide a solid scientific footing for the design and ongoing upkeep of road networks within saline soil environments. Analyzing prolonged monitoring data across diverse highway subgrades within a prototypical saline soil locale, we unveil the intricate temporal fluctuations and environmental sensitivities of the soil's mechanical properties under continuous load. Precisely, the subgrade's compressive modulus dwindled by 15%, while shear strength declined by 8% over a five-year period. These trends intensify during rainy and scorching seasons, with drops surpassing 20% and 12% respectively. Leveraging this intricate data, we deploy nonlinear regression analysis and

European Journal of Computational Mechanics, Vol. 33_5, 483–506.
doi: 10.13052/ejcm2642-2085.3353

sophisticated machine learning algorithms to construct a predictive model tailored for the long-term mechanical properties of fine-grained saline soil roadbeds. This model integrates a multitude of factors, including load duration, temperature, humidity, and more, delivering accurate forecasts of key subgrade indicators like compressive modulus, shear strength, and beyond. In the verification stage, compared with the measured data, the error rate of the model prediction results is controlled within 5%, showing high prediction accuracy and stability. In addition, we also carried on the sensitivity analysis to the model, found that the load size and the duration of the impact on the mechanical properties of the roadbed is the most significant. Therefore, in the design of road engineering in saline soil areas, the influence of these factors should be fully considered, and reasonable engineering measures should be taken to ensure the safety and durability of roads. This study not only provides effective data support for the long-term mechanical performance evaluation of fine-grained saline soil roadbed, but also provides an important theoretical reference for engineering practice in related fields.

Keywords: Fine-grained saline soil, mechanical properties, predictive models, modulus of compression.

1 Introduction

In arid and semi-arid regions, soil salinization emerges as a formidable challenge, fueled by heightened evaporation rates, drastic temperature fluctuations, and scarce rainfall. This phenomenon, along with groundwater alkalization, serves as ominous harbingers of land desertification, posing pressing global concerns. Globally, saline soils encompass a staggering 1 billion hectares, while in China alone, they sprawl across an immense 900,000 square kilometers. Within China, saline soils are broadly categorized into inland and coastal types, with Xinjiang's inland saline soils occupying a particularly prominent position. Strategic and judicious management of these soils in Xinjiang, a pivotal node along the Belt and Road Initiative, holds immense potential to propel infrastructure advancements and foster regional development.

However, in Northwest China, due to the special environmental conditions in this area, such as dry climate, low rainfall and great temperature difference, large evaporation, extremely high mineralization and serious secondary salinization, A vast area of coarse-grained saline soil emerged here, where salt expansion and deformation occur due to phase transitions

of soluble salts triggered by temperature variance, rainfall, and evaporation, which can easily cause cracking and uneven settlement of highways, railways and buildings [1, 2], which directly affects the rational application of coarse-grained saline soil in this area. During engineering design and construction in these areas, engineers and technicians often dispose of coarse-grained saline soil because of the engineering harm of saline soil, which leads to a huge amount of discarded soil and seriously destroys the local water and soil conservation and ecological balance [3, 4]. In view of the widespread distribution of coarse-grained saline soil and serious secondary salinization in Northwest China, how to effectively use large-scale natural coarse-grained saline soil as roadbed fillers has become an urgent geotechnical engineering problem for road construction in Northwest China under the premise of preventing road diseases in saline soil areas.

The term "coarse-grained saline soil" was first put forward by domestic expert Gao Shusen and others in the early 1990s when they studied the physical and mechanical properties of saline soil in northwest areas such as Xinjiang and Gansu. Subsequently, Hua Zunmeng, Luo Bingfang, Ding Zhaomin and other scholars have successively conducted relevant experimental studies on the engineering performance of coarse-grained saline soil applied to subgrade [5, 6]. However, there is still no unified standard to define coarse-grained saline soil. According to the "Technical Code for Construction of Saline Soil Areas", after saline washing, the saline soil named as coarse-grained soil by the graded grain size of soil samples can be considered as coarse-grained saline soil. However, the grain size limit value of coarse-grained soil is not clear. The kosher salt soil referred to in engineering generally refers to gravel soil or sandy soil, whose particle size is greater than or equal to 2 mm, its mass exceeds 50% of the total mass, and its total salt content is more than 0.3% [7, 8].

As a kind of special soil, saline soil is very different from ordinary plain soil. One is that soluble salts can exist in soil in both solid and liquid forms. The second is that when the water content of saline soil increases, the state of soluble salt in the soil changes, resulting in changes in physical and mechanical properties of the soil, and a significant decrease in soil strength; Third, with the decrease of ambient temperature or humidity, the salt in the void of the soil concentrates and combines with the water molecules to produce crystallization, resulting in the expansion and deformation of the saline soil foundation; Fourthly, when the foundation of saline soil is submerged, the cemented crystalline salt in the soil is partially or completely dissolved by water, thereby reducing the cementation ability between soil

particles, resulting in the destruction of saline soil. When the soil particles slide each other, the soil voids will gradually decrease and the soil will sink; Fifth, due to the existence of soluble salts in soil, they not only corrode concrete and metallic materials in building structures, but also affect the safety and stability of infrastructure such as roads and railways.

Numerous methodologies exist for categorizing saline soils, each rooted primarily in the soil's inherent characteristics, such as the nature of salts present, their concentration, and the solubility challenges they pose in water. Additionally, classifications are often tailored to the degree of harm and influence these soils exert on industries, agriculture, and transportation. For instance, in agriculture, where the growth of conventional crops is adversely affected, saline soils are classified based on the composition and concentration of soluble salts. Conversely, in engineering contexts, classifications consider the impact on project utilization, thereby tailoring the categorization to the specific needs and challenges of the engineering domain.

Different engineering types are affected by saline soil characteristics and damage degree is not the same, such as road and railway roadbed affected by saline soil is very different from the foundation and foundation of housing construction, so each industry department can classify saline soil according to its own characteristics and needs [9, 10]. In addition, special attention should be paid to the fact that the classification of saline soil needs to consider many factors and different starting points, so far there is no unified standard method for classification of saline soil.

2 Study on Salt Expansion Characteristics of Coarse-grained Saline Soil

2.1 Analysis on Mechanism of Salt Expansion and Its Influencing Factors

When the temperature decreases, sodium sulfate saline soils will produce volume expansion, and part of the deformation is due to salt heaving caused by the water-absorbing crystallization of Na_2SO_4 in the soil, and the other part is due to the frost heaving deformation of free water [11]. Salt heaving occurs above 0°C, while below 0°C both salt and frost heaving jointly cause deformation, exhibiting a coupling effect [12]. During the process of salt heaving, the migration of water and salt in the soil will cause heat migration. Na_2SO_4 solution will absorb 10 water molecules to form Glauber's salt crystals ($Na_2SO_4 \cdot 10H_2O$), and the volume will expand about 3.18 times [13].

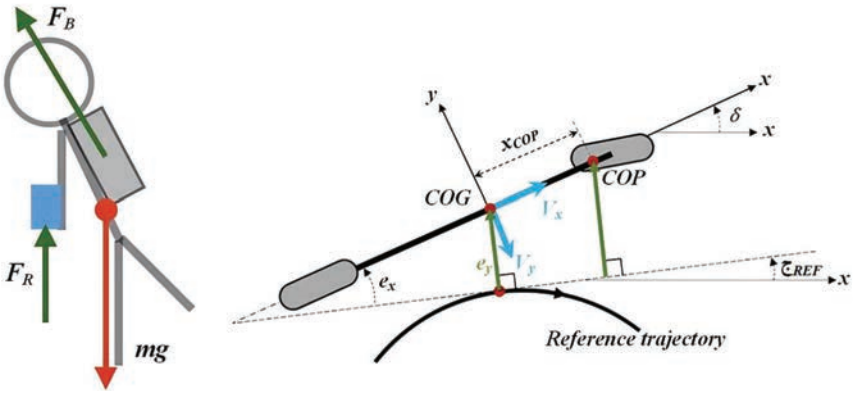

Figure 1 Evolution diagram of long-term compressive strength of fine-grained saline soil subgrade.

Figure 1 shows evolution diagram of the long-term compressive strength of fine-grained saline soil subgrade. At the same time, free water freezes into ice crystals at low temperature. The prevalence of salt-frost heaving significantly contributes to the uneven deformation of saline soil roadbeds, resulting in surface waves, bulges, and substantial degradation of the roadway. This saline soil deformation can be meticulously divided into three distinct processes, each defined by specific temperature thresholds [14]. These stages encompass: pure salt heaving that occurs above 0°C, where the solubility curve of anhydrous sodium sulfate inversely correlates with rising temperatures, leading to Na_2SO_4 crystallization from the salt solution and subsequent soil volume expansion; salt-frost heaving within a defined subzero temperature range; and pure frost heaving at even lower temperatures. Below 0°C, the formation of ice crystals in the salt solution reduces the availability of free liquid water, escalating the solution's salt concentration and fostering the crystallization of Glauber's salt. Concurrently, during the freezing process, Na_2SO_4 molecules precipitate from the ice crystals, further contributing to the deformation. At this time, the frost heaving effect promotes the further occurrence of salt heaving deformation. Furthermore, during the formation of $Na_2SO_4 \cdot 10H_2O$, Na_2SO_4 molecules absorb 10 water molecules from the salt solution, thereby reducing the amount of unfrozen water. This process, known as salt heaving, partially inhibits frost heaving. However, as temperatures continue to plummet, frost heaving becomes more prominent, dominating over salt heaving since Na2SO4 within ice crystals cannot absorb free water. The Uzan model and the octahedral shear stress

model are shown in (1) and (2).

$$M_R = k_1 \theta^{k_2} \sigma_d^{k_3} \tag{1}$$

$$M_R = k_1 p_a \left(\frac{\theta}{p_a} \right)^{k_2} \left(\frac{\tau_{oct}}{p_a} \right)^{k_3} \tag{2}$$

Generally speaking, the solubility of most soluble salts diminishes with falling temperatures. When the concentration of salt solution in the soil falls below its solubility threshold, debris precipitates from the solution. If the volume of this debris exceeds the original unsaturated salt solution, the soil experiences salt expansion. Additionally, when temperatures dip below the soil's freezing point, frost heaving occurs, and the combined effect of salt and frost heaving exerts a comprehensive impact on the soil. There are many factors affecting salt heave. The temperature change function on the boundary surface and the overall stiffness matrix are shown in (3) and (4).

$$T(t) = T_0 + \alpha t + Asin \left(\frac{2\pi t}{8640} + \frac{\pi}{2} \right) \tag{3}$$

$$[K] = \sum_{e=1}^{n} [K]^e = \sum_{e=1}^{n} [B]^T [D][B] dA \tag{4}$$

The pivotal factors influencing salt heave deformation in saline soil, as recognized by scholars globally, encompass soil quality, temperature, salt content, humidity, particle size distribution, density, and applied loads. Notably, coarse-grained saline soil exhibits weaker salt-frost heave characteristics due to its higher porosity compared to fine-grained soils. Furthermore, chloride salts exhibit a unique chemistry that melts ice, thereby lowering the freezing point and exhibiting a mitigating effect on soil salt frost heave. Conversely, sulfates are the primary driver of salt heave deformation [15]. Among the culprits for roadway deterioration in saline soil regions, salinity, moisture, and soil temperature are paramount. However, the harm inflicted by these factors can be mitigated or even negated through human intervention. Thus, the cornerstone of eliminating and preventing saline soil roadbed maladies lies in strategically managing the controllable factors within roadbed fillings, particularly salt content, moisture levels, and soil temperature.

2.2 Lab Salt Expansion Test of Coarse-grained Saline Soil

Coarse-grained saline soil differs from fine-grained in salt expansion, due to its large pores. As temperature drops, $Na_2SO_4 \cdot 10H_2O$ crystals formed

Table 1 Basic physical property parameters

Source of Soil Sample	d <2 mm	d <20 mm	W_{opt}	Gradation State	Soil Sample Classification
Urumqi	25.65	100	5.1	Good gradation	Coarse grained soil

from soil's Na_2SO_4 absorb water, filling macropores between particles. Accumulating Glauber's salt affects soil particles, triggering salt expansion. To clarify its mechanism and evolution in coarse-grained saline soil roadbeds, salt expansion tests are essential. The Mohr-Colunb strength criteria and the incremental stress-strain relationship expressions are shown in (5) and (6).

$$f = \tau_n - c - \sigma_n tg\varphi = 0 \tag{5}$$

$$d\{\varepsilon\} = f(\{\sigma\}) \tag{6}$$

Due to sampling challenges in saline soils, controlling salt type/amount, humidity, and particle gradation is difficult [16, 17]. To precisely study salt expansion in coarse-grained saline soil, this paper uses lab-prepared soil. The original soil (salt $< 0.1\%$) serves as the base. Table 1 details its physical properties. Following China's code and Xinjiang's guidelines, we classify saline soil based on salinization, set NaCl and Na_2SO_4 limits, and blend well-graded coarse-grained saline soil to obtain soil with specified salt content.

2.3 Test Plan

(1) In the salt expansion test, Haier medical low-temperature control box (temperature range: $-40°C\sim -25°C$) is used to reduce the temperature step by step, and the temperature can be intelligently controlled and constant. The indoor temperature is 20°C.
(2) Electric compaction instrument, compaction cylinder and other equipment, which are the same as the compaction test of soil.
(3) Other measuring equipment such as porous bottom plate, load plate and dial gauge are basically consistent with the equipment stipulated in the soil bearing ratio (CBR) test in the "Highway Geotechnical Test Regulations".

Figure 2 presents a comprehensive analysis of the impact of salt content on the elastic modulus of fine saline soil. The specimens were meticulously prepared under 96% compaction, with variations in both salt and water concentrations. For each distinct salt level, a series of samples were crafted, each containing 4.0%, 5.1%, and 6.0% moisture content, ensuring a robust dataset

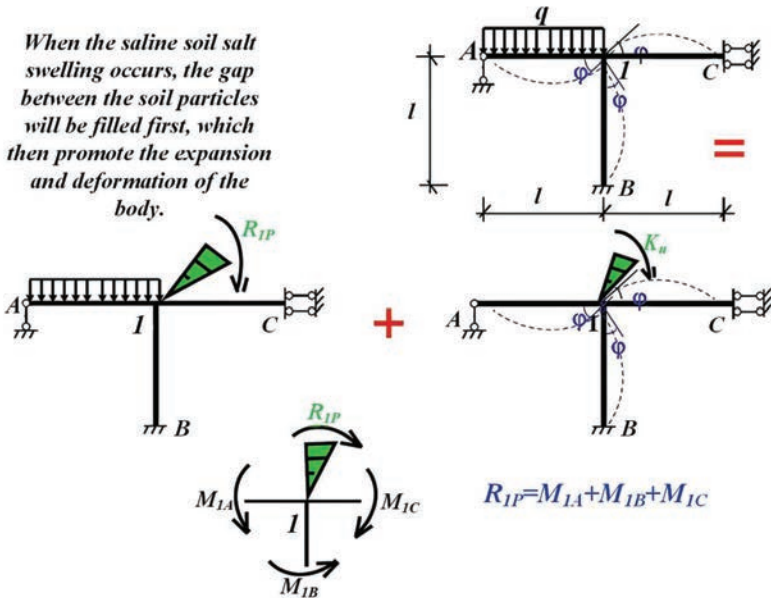

Figure 2 Analysis of salt content on elastic modulus of fine saline soil.

with three parallel samples per group. The figure further illustrates the plastic potential function and its incremental form, as expressed in Equations (7) and (8), respectively, providing a mathematical framework for understanding the intricate relationships at play.

$$G = \alpha' I_1 + \sqrt{J_2} - K' = 0 \tag{7}$$

$$dH_\alpha = \{\sigma\}^T \{d\varepsilon_p\} \tag{8}$$

(1) After the sample is formed, remove the damaged filter paper on the top surface of the sample and replace it with a good filter paper.

(2) Considering the self-weight of the subgrade soil and the effect of the overlay load of the pavement structure, four load plates (1.25 kg each) are added to the upper part of the porous plate with adjusting bars, which is about 3.2 kPa.

(3) Tighten the pull rods on both sides of the compaction cylinder with a wrench, and install the dial gauge on the bracket. After checking, put the test cylinder, the dial gauge and the porous plate into the low temperature control box together. Figure 3 shows prediction model of long-term creep behavior of fine-ained saline soil subgrade.

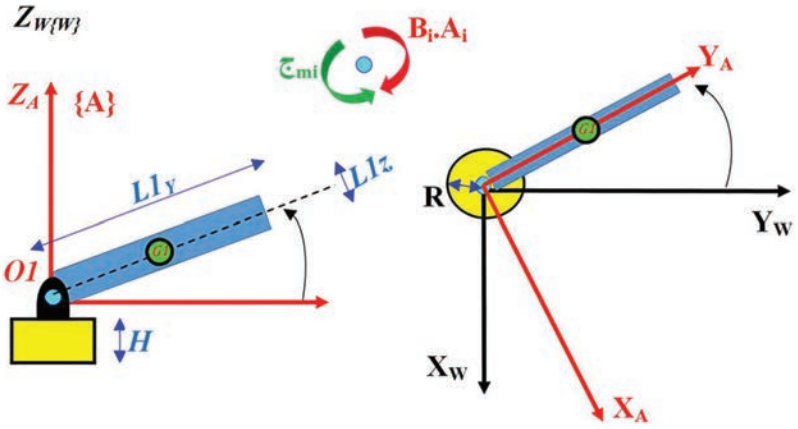

Figure 3 Prediction model of long-term creep behavior of fine-ained saline soil subgrade.

(3) Salt expansion monitoring

(1) Adjust the temperature of the low temperature control box to 20°C and keep the temperature constant for 24 hours.
(2) The next day, read the initial reading of the dial meter and record it.
(3) To conduct the experiment, the temperature within the low-temperature control box is to be systematically decreased from +20°C to −30°C, with each decremental stage involving a 5°C reduction. Upon reaching each intermediate temperature, the system is maintained at a constant state for 120 minutes to ensure stability. Subsequently, the final reading of the dial meter, influenced by this specific temperature, is recorded. Furthermore, throughout this temperature range, the salt expansion value is meticulously documented for comprehensive analysis.

3 Analysis of Experimental Results

3.1 Salt Expansion Characteristics of Coarse-grained Sulfate Saline Soil

Figure 4 shows the relationship between the salt expansion and the temperature of the coarse saline soil with different salt content at the specific compaction degree and water content. As the temperature decreases, the soil first slightly shrinks due to the large pore structure, then the sodium

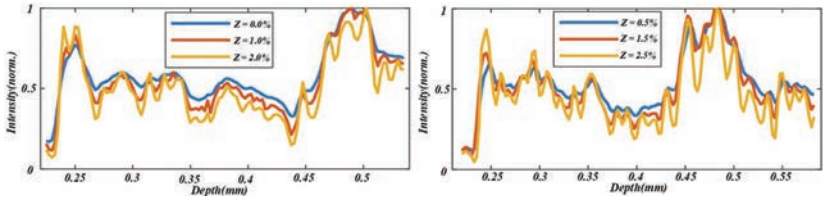

Figure 4 Relationship between salt expansion and temperature of coarse-grained sulfate saline soil with different salt content when water content $\omega = 5.1\%$.

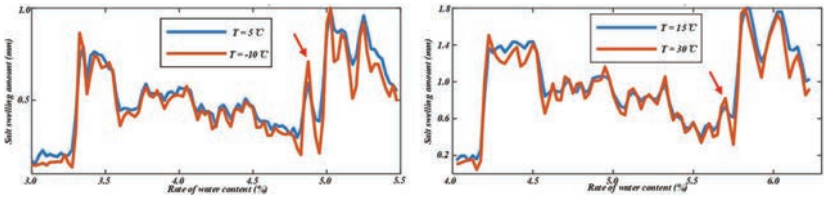

Figure 5 Relation curve of soil salt swelling and temperature at different temperatures.

sulfate crystals increase, and the volume increases to a stable state [18]. The maximum salt expansion amount was 2.40 mm. The salt swelling of samples with salt content greater than 1.5% is sensitive to temperature. The sensitive temperature of salt swelling is mainly between 15°C and −20°C, and the incipient swelling temperature is 15°C, and the swelling of coarse-grained sulfate saline soil is more violent under the temperature environment of −15°C to 10°C.

Figure 4 vividly demonstrates that upon reaching temperatures ranging from −25°C to −20°C, salt heave attains a state of stability across various salt concentrations. This stabilization can be attributed to the dual nature of salt heave, which encompasses both salt expansion and frost heave. At warmer temperatures, salt expansion predominates, driving the heave process. However, as temperatures plummet below −25°C, soil moisture transforms into ice crystals, thereby diminishing the available water pool. Consequently, supersaturated sodium sulfate finds itself unable to absorb sufficient water [19], causing frost heave to assume primacy. This shift results in a gradual leveling off of the salt heave curve, a phenomenon that aligns seamlessly with established research findings.

Figure 5 shows the relation curve of soil salt swelling and temperature at different temperatures. The volume of coarse-grained soil exhibits a slight decrease with increasing water content above 0°C. However, below 0°C, the soil volume increases with rising water content. For coarse-grained saline

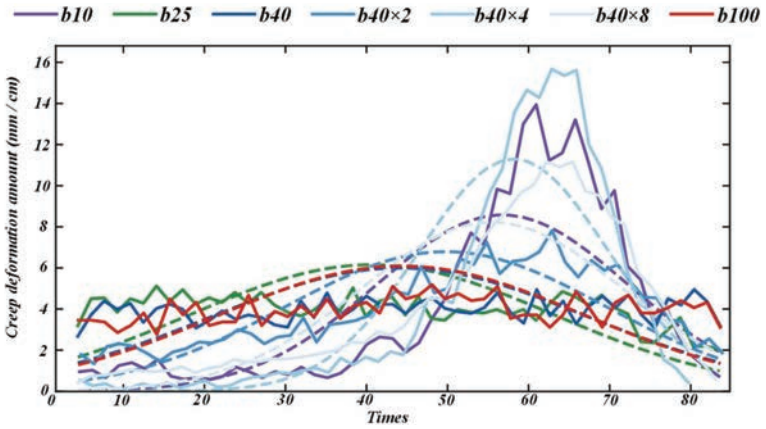

Figure 6 Creep characteristic curve of fine-grain saline soil subgrade.

soil, salt expansion initially rises and then falls with increasing moisture, peaking at the optimal water content, regardless of temperature. This is because the volume of coarse-grained soil shrinks because of the increase of moisture in coarse-grained soil and the continuous discharge of gas; With the temperature falling below 0°C, the water in the pores of the soil gradually freezes and produces frost heave, resulting in the volume of the soil gradually increasing. For the coarse-grained saline soil, it can achieve better compactness under the state of the best moisture content, and the soil void formed on both sides of the best moisture content is relatively large [20, 21].

Figure 6 presents the creep characteristic curve of a fine-grained saline soil subgrade, elucidating a crucial aspect of its behavior. The graph reveals that under varying humidity conditions and temperatures, the salt expansion of coarse-grained sulfate saline soil intensifies proportionally with the increase in salt content. This underscores the pivotal role of salt as the primary catalyst for salt heaving, as a higher concentration of sodium sulfate fosters the formation of more Glauber's salt crystals upon water absorption. Furthermore, when excess free water falls below 0°C, it undergoes freezing and contributes to additional heaving. The combined effects of salt and frost heaving amplify soil expansion significantly [22], corroborating established research findings. Notably, at a moisture content of 6.0%, the soil's higher water content and reduced air pockets facilitate a dominant role for frost heave. Conversely, at low salt levels ($Z = 0.5\%$), limited water absorption and crystallization fail to adequately fill the interstitial spaces between soil particles. Additionally, as temperature-induced shrinkage intensifies, the

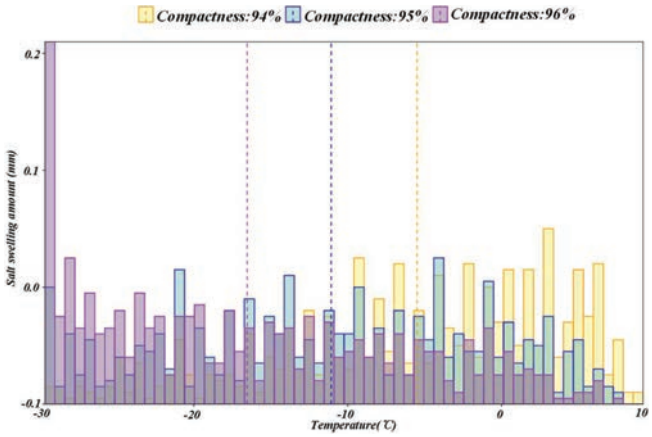

Figure 7 Relationship between salt expansion and temperature of coarse-grained chlorine saline soil with different salt content when water content $\omega = 5.1\%$.

initial phase of soil salt heave appears to be mitigated, further elucidating the intricate interplay between soil composition, moisture, and temperature.

3.2 Characteristics of Salt Expansion in Coarse Chlorine Saline Soil

Figure 7 shows the relationship between salt expansion and temperature of coarse-grained chlorine saline soil with different salt content under the condition of 96% compactness and optimum moisture content. It can be seen from the curve law in the figure that under the temperature environment above 0°C, the volume of coarse-grained chlorine saline soil has almost no change, that is, no salt expansion deformation occurs. As the temperature decreases, the volume of non-saline soil (i.e. coarse-grained soil) begins to expand, the deformation increases first and then decreases, and finally is in a stable state, and the volume shrinkage appears at 15°C–0.04 mm. At the same time, coarse-grained soil produces violent volume expansion in the temperature range of −25°C to 0°C. The reason is that the water in the soil will freeze below 0°C and produce frost heave effect. For coarse-grained chlorine saline soil, when the temperature drops to −10°C, the soil begins to expand to a certain extent, and the deformation reaches a peak value of 0.15 mm at −30°C. The analysis shows that NaCl in saline soil has the effect of melting snow and ice, and the effect of melting ice of chloride salt is greater than that of frost heave in the range of −20°C–0°C, and the soil almost does not produce swelling deformation; As the temperature continues

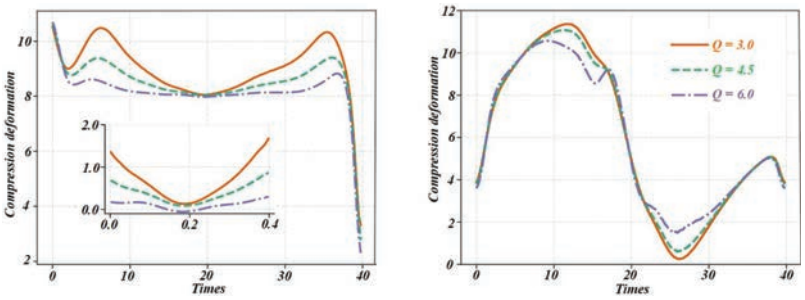

Figure 8 Compression deformation of fine saline soil.

to decrease, the frost heave effect becomes more and more obvious in the range of $-20°C\sim -40°C$, and the soil mass appears a certain amount of expansion deformation, showing a phenomenon of first increasing and then decreasing.

At a compaction level of 96%, the intricate interplay between salt expansion and water content in coarse-grained chlorine saline soil, across varying temperatures and salt concentrations, is elegantly portrayed through a meticulously crafted curve. This graphical representation captures the dynamic relationships at hand, offering valuable insights into the soil's behavior under different conditions.

Figure 8 illustrates the compression deformation characteristics of fine saline soil, revealing a subtle yet discernible trend. Specifically, the deformation of coarse-grained chlorine saline soil exhibits minimal fluctuations in response to variations in water content, with an overall downward trajectory [23]. This phenomenon stems from the fact that an increase in water content facilitates the dissolution of excess salt bridges between soil particles, thereby dismantling the salt-induced skeletal structure within the soil matrix. Consequently, the gaps between soil particles widen, and under the combined influence of soil weight and overlying loads, the soil undergoes compaction, manifesting as a gradual reduction in volume.

4 Study on Mechanical Properties of Coarse-grained Saline Soil

The difference between coarse-grained saline soil and ordinary coarse-grained soil is not simply the difference between the presence or absence of salt, but the change of its mechanical properties (i.e. road performance indicators) affected by water and salt. With the rapid development and

massive construction of infrastructure such as expressways and railways in Northwest China, there is a lack of high-quality embankment filling materials when building embankments in saline soil areas, and all embankments are replaced with sand and gravel materials, which will increase the cost of highway construction [24, 25]. The NCHRP 1-28A model and the Superpave performance model are shown in (9) and (10).

$$T_R = k_1 p_a \left(\frac{\theta - 3k_4}{p_a}\right)^{k_2} \left(\frac{\tau_{oct}}{p_a}\right)^{k_3} \tag{9}$$

$$Q = k_1 p_a \left(\frac{\theta}{p_a}\right)^{k_2} \left(\frac{\tau_{oct}}{p_a} + 1\right)^{k_3} \tag{10}$$

When saline soil is used as subgrade filler, its pavement performance is not only related to whether it can have a good application performance, but also the first factor to judge whether this kind of material can be used as subgrade filler [26]. Resilience modulus and CBR (California Bearing Ratio) are commonly used to assess pavement performance of subgrade fillings [27]. CBR, introduced by the California Highway Bureau, reflects local load and deformation resistance of roadbed materials [28]. Resilience modulus characterizes elastic deformation of subgrade soil, indicating the ratio of stress to strain under load, thus assessing vertical deformation resistance. The continuous conditions of the heat flow at the interface of the phase transition are shown in (11) and (12).

$$\frac{\partial}{\partial x}\left(\lambda \frac{\partial T}{\partial x}\right) + \frac{\partial}{\partial y}\left(\lambda \frac{\partial T}{\partial y}\right) = \rho c \frac{dT}{dt} \tag{11}$$

$$\left(\lambda_f \frac{\partial T}{\partial t} - \lambda_u \frac{\partial T}{\partial t}\right)_{(x,y)\in S(t)} = L^* \rho \frac{dS(t)}{dt} \tag{12}$$

This metric has gained widespread application in road design. Due to the complexity of dynamic triaxial test and the scarcity of dynamic triaxial testers, the application of dynamic modulus of resilience directly to evaluate the deformation performance of roadbed fillings is less popular. By establishing the relationship model between the load-bearing ratio (CBR) of embankment fillings and the dynamic resilience modulus, the method which can effectively estimate the dynamic resilience modulus based on the load-bearing ratio of embankment fillings has significant advantages. The Newman boundary function and the convection heat exchange boundary conditions

formula are shown in (13) and (14).

$$q = -\lambda \cdot \frac{\partial T}{\partial n} = q(x, y, t) \tag{13}$$

$$-\lambda \cdot \frac{\partial T}{\partial n} = B \cdot (T_a - T) \tag{14}$$

Extensive research conducted globally and domestically has predominantly focused on the pavement performance of subgrade fill materials, emphasizing the load-bearing ratio (CBR) and static elastic modulus of non-saline soils. However, a notable gap exists in the investigation of the pavement performance of subgrade soils impacted by salinity, resulting in a disconnect between the anti-deformation capabilities of saline-affected subgrades and their actual load-bearing capacities. Given the ubiquitous presence of saline soil in our country, a thorough understanding of its pavement performance is paramount in assessing its feasibility as a roadbed filler material. Consequently, conducting thorough research on the road performance of saline soil is imperative to scientifically justify the feasibility of employing coarse-grained saline soil as roadbed filler in Northwestern China. Focusing on coarse-grained chlorine- and sulfate-saline soils, this chapter examines their rebound modulus and CBR under varying stress, water, and salt conditions using triaxial and CBR tests. It explores factors affecting their road performance and proposes a correlation between CBR and dynamic rebound modulus. A prediction model for the dynamic rebound modulus is introduced, offering an evaluation criterion for coarse-grained saline soil roadbed filling control.

4.1 CBR Test of Coarse-grained Saline Soil

To study the evolution of dynamic modulus and CBR in coarse-grained saline soil with varying water and salt contents, specimens were prepared at 96% compaction, with salt content and moisture (4.0%, 5.1%, 6.0%) varied. Each group had 3 parallel samples. CBR test specimens were crafted following China's geotechnical testing regulations, using a 152 mm-diameter, 170 mm-height compaction cylinder. Samples were prepared at optimal water content, targeting compaction by mass/volume. A comparative test group with $\omega_{opt} \pm 1\%$ moisture content analyzed the effect of humidity on CBR. The influence formula of salt content on strength and the long-term creep

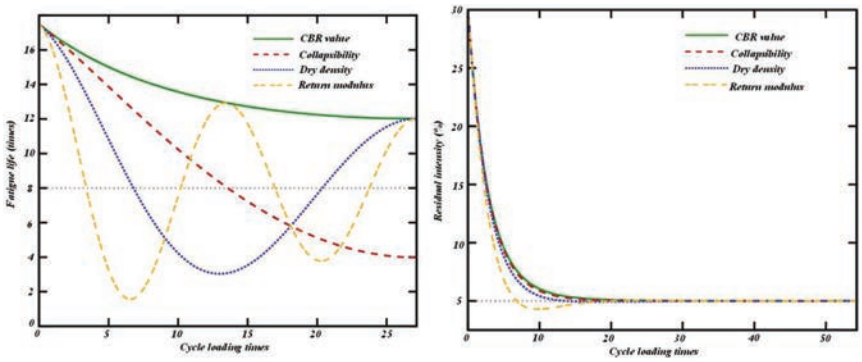

Figure 9 Forecast of fatigue life of fine-grain saline soil subgrade.

deformation prediction formula are shown in (15) and (16).

$$q_u = a - b \cdot S \tag{15}$$

$$\varepsilon_c = c \cdot \left(\frac{\sigma}{\sigma_y}\right)^n \cdot t^m \tag{16}$$

The penetration apparatus boasts a standardized rod dimension of H $\times$ D = 100 mm $\times$ 50 mm, capable of enduring a maximum load capacity of 30 kN and operating at a precise lifting speed of 1 mm/min. Moreover, it necessitates the utilization of supplementary measurement tools, encompassing three dial gauges along with their mounting brackets, four individual load plates each weighing 1.25 kg, and porous plates for accurate testing. The quantitative relationships governing the impact of humidity on long-term strength degradation and the influence of temperature on creep rate are succinctly represented in Equations (17) and (18), respectively.

$$w^2(t) = \Phi(t)\sigma_1^2 + \Psi(t)\sigma_2^2 \tag{17}$$

$$r = \sum_{k=1}^{m-1} |d_{k+1} - d_k|/(m-1) \tag{18}$$

Figure 9 shows forecast of fatigue life of fine-grain saline soil subgrade. According to the calculation and value of load-bearing ratio (CBR) stipulated in the newly promulgated "Highway Geotechnical Test Regulations" in our country, the CBR (in percentage) is calculated for both 2.5 mm and 5.0 mm

penetration, and the higher value is adopted as the load-bearing ratio (CBR) for coarse-grained saline soil. The specific calculation methods are shown in formula (19) and formula (20):

$$CBR_{2.5} = \frac{P_{2.5}}{7000} \times 100 \tag{19}$$

$$CBR_{5.0} = \frac{P_{5.0}}{10500} \times 100 \tag{20}$$

This paper measures the CBR of coarse-grained saline soil at optimal moisture (ω_{opt}) and $\omega_{opt} \pm 1\%$ to assess the impact of humidity on its CBR value.

4.2 Test Results and Analysis

At a compaction degree of 96%, under varying humidity and settlement conditions, the penetration depth of coarse-grained saline soil with different salt contents increases nonlinearly for low salt (Z $<$ 2.0%) and approximately linearly for high salt (Z $>$ 2.0%) as the unit compressive stress increases. As salt content rises from 2.0% to 8.0%, the permeability of identically compacted samples in water increases, while the vertical compression stress of coarse-grained saline soil with varying humidity decreases significantly when penetrated 5.0 mm, ranging from 13.89%–66.07%. This suggests lower salt content leads to weaker permeability and lesser impact.

Figure 10 vividly illustrates the shear strength behavior of saline soil subgrade across varying humidity levels. Notably, at a compaction level of 96%, the California Bearing Ratio (CBR) of coarse-grained saline soil exhibits a discernible decline in correlation with increasing water content, irrespective of salt concentration. Furthermore, the figure highlights that for a given water content, the CBR values attained at a 5 mm penetration depth surpass those measured at 2.5 mm, underscoring the sensitivity of CBR to penetration depth.

Figure 11 shows stress-strain response of the subgrade at different loading rates. Analysis of test results reveals that higher salt content in coarse-grained saline soil leads to lower CBR after water immersion. Data shows sulfate soil with low salt has higher CBR than high-salt chloride soil under identical conditions. Additionally, sulfate soil's CBR response to stress, water, and salt is similar to chloride soil.

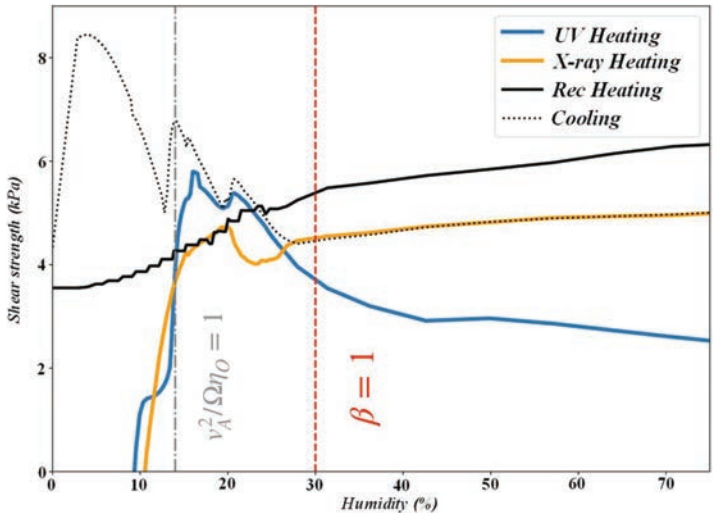

Figure 10 Shear strength of saline soil subgrade under different humidity.

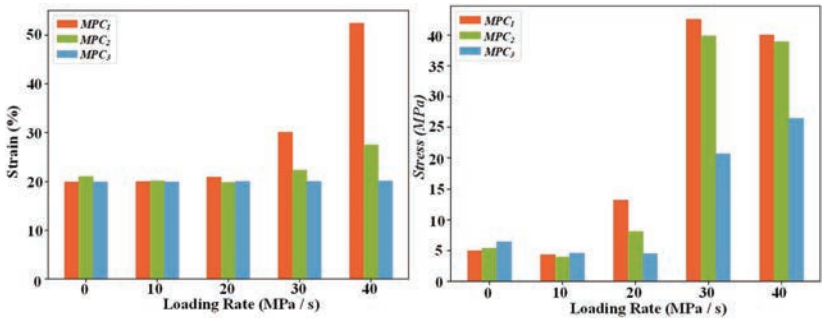

Figure 11 Stress-strain response of subgrade at different loading rates.

5 Conclusion

This research meticulously assesses the long-term mechanical attributes of fine-grained saline soil subgrades, culminating in the development of a predictive model that accurately forecasts their behavior. Through a meticulous examination of extensive long-term monitoring data, we have garnered a profound comprehension of the temporal evolution of these subgrades' performance. Our findings reveal that, over a five-year observational period, the compressive modulus of fine-grained saline soil subgrades experienced a noteworthy average reduction of 15%, while the shear strength declined by

an average margin of 8%. These quantitative insights emphasize the proclivity of saline soil subgrades to undergo performance deterioration under the influence of sustained loading conditions. Especially, in rainy season and high temperature season, due to the change of humidity and temperature, the performance index of roadbed decreases by 20% and 12% respectively, which indicates that environmental factors have a significant impact on the performance of saline soil roadbed. Based on these data, we use nonlinear regression analysis and machine learning algorithms to build a predictive model. The model can synthetically consider many factors such as load time temperature humidity and so on and accurately predict the compressive modulus shear strength and other key indicators of subgrade. The verification results show that the prediction error rate of the model is controlled within 5%, showing extremely high prediction accuracy and reliability. Through this study, we draw the following conclusions: firstly, the performance of fine-grained saline soil roadbed has obvious degradation phenomenon under long-term load, especially in rainy season and high temperature season; Secondly, the prediction model we constructed can accurately predict the long-term mechanical properties of saline soil subgrade, which provides strong support for the design and maintenance of road engineering. In conclusion, this study not only provides important data support for the long-term mechanical performance evaluation of fine-grained saline soil roadbed, but also provides an effective theoretical reference for engineering practice in related fields. In the future, we will continue to optimize the prediction model, improve the prediction accuracy, and make greater contributions to the road construction in saline soil areas.

Funding

Natural Science Foundation of Xinjiang Uygur Autonomous Region (2022D01A56); Tianshan Talent Training Program (2023TSYCLJ0055).

References

[1] Akbari, P., Zamani, M., and Mostafaei, A. Machine learning prediction of mechanical properties in metal additive manufacturing. Additive Manufacturing, vol. 91, pp. 104320, 2024.

[2] Han, J., Dong, G., Li, S., Zheng, J., Wang, J., Li, H., Starostenkov, M. D., and Bi, J. Uneven distribution of cooling rate, microstructure and

mechanical properties for A356-T6 wheels fabricated by low pressure die casting. Journal of Manufacturing Processes, vol. 127, pp. 196–210, 2024.

[3] Huo, X., Wang, P., Wang, S., Guo, R., and Wang, Y. Experimental study on the mechanical properties and impermeability of basalt-PVA hybrid fibre reinforced concrete. Case Studies in Construction Materials, vol. 21, pp. e03646, 2024.

[4] Kong, Z., Wang, X., Hu, N., Jin, Y., Tao, Q., Xia, W., Lin, X.-M., and Vasdravellis, G. Mechanical properties of SLM 316L stainless steel plate before and after exposure to elevated temperature. Construction and Building Materials, vol. 444, pp. 137786, 2024.

[5] Li, H., Wei, Y., Du, H., Chen, J., and Zhang, Y. Comparative experimental investigation on mechanical properties of bamboo scrimber and SPF. Structures, vol. 67, pp. 106993, 2024.

[6] Miao, X., Hu, J., Xu, Y., Su, J., and Jing, Y. Review on mechanical properties of metal lattice structures. Composite Structures, vol. 342, pp. 118267, 2024.

[7] Pradeep, V., Kumar, P., and Reddy, I. R. Investigation on mechanical properties and wear behavior of basalt fiber and SiO2 nanofillers reinforced composites. Results in Engineering, vol. 23, pp. 102722, 2024.

[8] Sadeghzadeh, S., Badrinezhad, L., and Eshkalak, K. E. Mechanical properties of C3N-BN hybrid nanosheets: Insights from molecular dynamics simulations. Diamond and Related Materials, vol. 147, pp. 111323, 2024.

[9] Shao, K., Zhen, Z., Gao, R., Song, M., Zhang, L., and Zhang, X. Comparative experimental study of the effect of loading rate on the typical mechanical properties of bubble and clear ice cubes. Experimental Thermal and Fluid Science, vol. 159, pp. 111264, 2024.

[10] Sohrabian, M., Vaseghi, M., Eslamloo, S. R., Sameezadeh, M., Arab, B., and Moradi, F. Molecular dynamics study on mechanical properties of polycaprolactone/bioactive glass nanocomposites. Computational Materials Science, vol. 243, pp. 113098, 2024.

[11] Wang, B., Li, N., Bao, Q., Cheng, S., Feng, J., Li, M., Wang, N., Wang, Z., Jiang, B., Chen, L., Hong, H., and Jian, X. Graphene at different scales to synergistically optimize the thermal and mechanical properties of CF/PPBESK composites. Composites Part B: Engineering, vol. 284, pp. 111692, 2024.

[12] Wang, Y., Zhang, Q., Pan, N., Xu, Y., Lu, D., Cai, J., and Feng, J. Mechanical properties of hoberman radially retractable roof structures. Thin-Walled Structures, vol. 203, pp. 112176, 2024.

[13] Wang, Z., Bai, E., Liang, L., Du, Y., and Liu, C. Comparison of dynamic mechanical properties of carbon fiber and graphene oxide grafted carbon fiber modified concrete. Journal of Building Engineering, vol. 94, pp. 109989, 2024.

[14] Bai, Y., Arulrajah, A., Horpibulsuk, S., and Zhou, A. Geopolymer stabilization of carbon-negative gasified olive stone biochar as a subgrade construction material. Construction and Building Materials, vol. 442, pp. 137617, 2024.

[15] Chen, J., Zhang, Y., Hou, Y., and Han, B. Study on mechanical properties and microstructure of improved saline soil subgrade filler. Case Studies in Construction Materials, vol. 20, pp. e03014, 2024.

[16] Cui, G., Liu, Z., Ma, S. xian, and Cheng, Z. Dynamic characteristics of carbonate saline soil under freeze–thaw cycles in the seaonal frozen soil region. Alexandria Engineering Journal, vol. 81, pp. 384–394.

[17] Hao, J., Cui, X., Bao, Z., Jin, Q., Li, X., Du, Y., Zhou, J., and Zhang, X. Dynamic resilient modulus of heavy-haul subgrade silt subjected to freeze-thaw cycles: Experimental investigation and evolution analysis. Soil Dynamics and Earthquake Engineering, vol. 173, pp. 108092, 2024.

[18] Liu, Z., He, Z., Zhang, W., and Luo, S. Laboratory test and prediction model of dynamic resilient modulus of carbonaceous mudstone coarse-grained soil. Case Studies in Construction Materials, vol. 18, pp. e01887, 2023.

[19] Niu, X., and Yao, Y. Resilient modulus experiment of subgrade soil on different wetting–drying and salt washing–supplying paths. Transportation Geotechnics, vol. 28, pp. 100512, 2021.

[20] Peng, S., Wang, F., Li, X., and Fan, L. Experimental research on employed expanded polystyrene (EPS) for lightened sulfate heave of subgrade by thermal insulation properties. Geotextiles and Geomembranes, vol. 48(4), pp. 516–523, 2020.

[21] Razouki, S. S., and Kuttah, D. K. Behaviour of fine-grained gypsum-rich soil under triaxial tests. Proceedings of the Institution of Civil Engineers – Construction Materials, vol. 174(5), pp. 240–248, 2019.

[22] Shah, R., and Mir, B. A. Effect of varying pore water salinity on frost susceptibility behaviour of soils. Transportation Geotechnics, vol. 35, pp. 100776, 2022.

[23] Shen, J., Wang, Q., Chen, Y., Zhang, X., Han, Y., and Liu, Y. Experimental investigation into the salinity effect on the physicomechanical properties of carbonate saline soil. Journal of Rock Mechanics and Geotechnical Engineering, vol. 16(5), pp. 1883–1895, 2024.
[24] Song, L., Chen, S., Wang, C., Wen, P., and Chen, H. Engineering properties on salt rock as subgrade filler in dry salt lake: Water retention characteristics and water migration patterns. Construction and Building Materials, vol. 406, pp. 133414, 2023.
[25] Wang, F., Peng, S., Fan, L., and Li, Y. Mechanism of pore relative humidity on salt swelling characteristics in sulfate saline soil. Alexandria Engineering Journal, vol. 61(6), pp. 4963–4976, 2022.
[26] Wang, Z., Zhu, J., and Ma, T. Review on monitoring of pavement subgrade settlement: Influencing factor, measurement and advancement. Measurement, vol. 237, pp. 115225, 2024.
[27] Ying, Z., Cui, Y.-J., Benahmed, N., and Duc, M. Salinity effect on the compaction behaviour, matric suction, stiffness and microstructure of a silty soil. Journal of Rock Mechanics and Geotechnical Engineering, vol. 13(4), pp. 855–863, 2021.
[28] Zhou, Z., Li, G., Shen, M., and Wang, Q. Dynamic responses of frozen subgrade soil exposed to freeze-thaw cycles. Soil Dynamics and Earthquake Engineering, vol. 152, pp. 107010, 2022.

Biographies

Ruheiyan Muhemaier is now a doctoral candidate at Xinjiang University. He is mainly engaged in ecological geology and disaster geology. Presided over 1 project of Natural Science Foundation of Xinjiang Uygur Autonomous Region, participated in 3 projects of natural Science Foundation, published more than 10 papers, and authorized 5 patents.

Mao Wei is a professor and senior engineer of Xinjiang Vocational and Technical College of Communications. He graduated from China University of Geosciences (Wuhan) with a PhD in Geological engineering. He is a master's supervisor of Xinjiang University. He is mainly engaged in research work in engineering geology, disaster geology and tunnel geotechnical.

Liu Xuejun is a senior engineer, Registered civil engineer, the first Master of Engineering Survey and Design in Xinjiang Uygur Autonomous Region, the Chinese Construction craftsman, the Outstanding Civil Engineer in Central and Western China, the leading scientific and technological innovation talent of "Tianshan Talents" in Xinjiang Uygur Autonomous Region, the chief expert, Deputy chief engineer and the head of the postdoctoral workstation of Xinjiang Academy of Building Science (Co., LTD.), Deputy General manager and Chief Engineer of Geotechnical Investigation Division, Director and chief scientist of Geotechnical Engineering Technology Research Center with Special Conditions in Xinjiang Uygur Autonomous Region.

Xie Liangfu, professor, Dean of the School of Civil Engineering and doctoral Supervisor of Xinjiang University, is engaged in the research of slope geological disaster prevention, geotechnical numerical simulation, underground engineering surrounding rock stability evaluation, etc. In the past five years, he has presided over 2 national natural science fund projects and 3 provincial and ministerial level projects, published 1 academic monographs, and published more than 20 high-level papers.

Ren Zulin graduated from Taiyuan University of Technology in June 2022, is currently a master's student in Civil Engineering at Xinjiang University, mainly engaged in research on the mechanical properties of special geotechnical engineering.